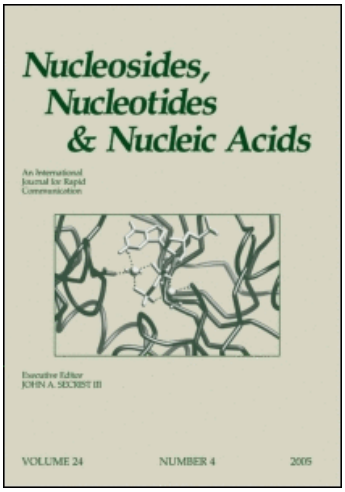

Nucleosides, Nucleotides and Nucleic Acids
Publication details, including instructions for authors and subscription information:
http://www.informaworld.com/smpp/title~content=t713597286

Steric Block High Affinity Oligonucleotide Analogues: A New Tool for Mapping RNA-Protein Binding Sites

Douglas Brown[a]; Emily Joy[a]; Jane Greatorex[a]; Michael J. Gait[b]; Andrew M. L. Lever[a]
[a] Department of Medicine, University of Cambridge, Addenbrookes Hospital, Cambridge, United Kingdom [b] MRC Laboratory of Molecular Biology, Cambridge, United Kingdom

To cite this Article Brown, Douglas , Joy, Emily , Greatorex, Jane , Gait, Michael J. and Lever, Andrew M. L.(2008) 'Steric Block High Affinity Oligonucleotide Analogues: A New Tool for Mapping RNA-Protein Binding Sites', Nucleosides, Nucleotides and Nucleic Acids, 27: 2, 196 — 212
To link to this Article: DOI: 10.1080/15257770701795961
URL: http://dx.doi.org/10.1080/15257770701795961

Nucleosides, Nucleotides, and Nucleic Acids, 27:196–212, 2008

ISSN: 1525-7770 print / 1532-2335 online
DOI: 10.1080/15257770701795961

Taylor & Francis
Taylor & Francis Group

STERIC BLOCK HIGH AFFINITY OLIGONUCLEOTIDE ANALOGUES: A NEW TOOL FOR MAPPING RNA-PROTEIN BINDING SITES

Douglas Brown,[1] Emily Joy,[1] Jane Greatorex,[1] Michael J. Gait,[2] and Andrew M. L. Lever[1]

[1]*Department of Medicine, University of Cambridge, Addenbrookes Hospital, Cambridge, United Kingdom*
[2]*MRC Laboratory of Molecular Biology, Cambridge, United Kingdom*

□ *Steric-block ON analogues are efficient inhibitors of RNA-protein interaction and therefore have potential to probe RNA sequences for putative protein binding sites and to investigate mechanisms of protein binding. The packaging process of HIV-1 is highly specific involving an interaction between the Gag protein and a conserved sequence that is only present on genomic viral RNA. Using oligonucleotide probes we have confirmed that the terminal purine loop is the major Gag binding site on SL3 and that a secondary Gag binding site exists at an internal purine bulge. We also demonstrate direct binding of oligonucleotide to their binding sites and confirm this interaction does not alter global RNA conformation, making them highly specific, nondisruptive probes of RNA protein interactions.*

Keywords High affinity oligonucleotide; RNA; Gag protein; binding; HIV

INTRODUCTION

High affinity oligonucleotide (ON) analogues have been utilized in a number of studies with applications ranging from *in vitro* mRNA degradation to therapeutic intervention. Broadly, ON analogues can be arranged into two groups: Ribonuclease H activating ONs and steric blocking ONs. ONs containing a central DNA region, flanked by higher affinity nucleotide analogues, can form a DNA-RNA hybrid with a specific RNA sequence, resulting in Ribonuclease H cleavage and destruction of the target RNA.[1,2]

Received 4 April 2007; accepted 23 August 2007.
We thank Donna Williams and Matthew Watson for synthesis of oligonucleotides. We are also grateful for the helpful advice on oligonucleotides from Andrey Arzumanov. This work was funded by a Medical Research Council grant G0400759.
Address correspondence to Andrew M. L. Lever, Department of Medicine, University of Cambridge, Addenbrookes Hospital, Hills Road, Cambridge, CB2 2QQ, UK. E-mail: amll1@mole.bio.cam.ac.uk

Steric-block ON analogues generally possess increased affinities for target RNA sequences, with binding resulting in the disruption of RNA processes and not RNA degradation.[3,4] Steric-block ONs can block gene expression by inhibiting RNA-protein interactions during a number of cellular processes including RNA splicing,[5] translation,[6] and transcription[7–12] and have shown promise as therapeutics.[13–17] The sequence specific nature of steric-block ONs, and the ability to use very short ONs, suggests they have potential as in vitro tools for identifying specific RNA sequences involved in protein binding and for investigating the relative role of multiple binding sites.

One possible target is the HIV-1 packaging signal (Ψ). Packaging of the retroviral dimeric RNA genome is a highly specific process requiring selection of full-length genomic viral RNA from a background of spliced viral transcripts and cellular mRNAs. This is achieved by the interaction of the Gag polyprotein with Ψ, present in the 5′-leader region of genomic RNA.[18,19]

In HIV-1, the core Ψ region contains four stem-loop sequences (SL1-4), the first three of which have defined roles in genomic RNA dimerisation, in splicing and in packaging, respectively.[20–23] The virally encoded Gag protein interacts with this region through two zinc fingers present in the nucleocapsid (NC) domain.[24,25] More specifically, this process involves interactions between the zinc fingers and G residues at position 771 and 773 (numbering based on the infectious molecular clone HIV-1 HXB2 [26]) of the SL3 sequence of Ψ (Figure 1A).[27] Deletion of SL3 causes a significant reduction in the level of viral RNA packaged.[20,28] Structural analysis suggests that an initial Gag-SL3 interaction results in unwinding of

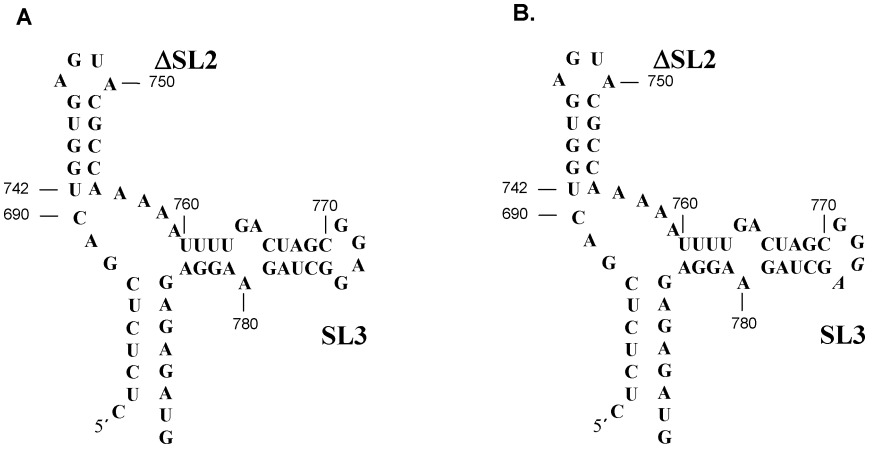

FIGURE 1 Target RNAs used in this study. **A.** ΔA1 RNA consisting of SL2 and SL3 with an SL1 deletion (Δ691–742). **B.** GGGA mutant RNA of the same sequence as ΔA1 except for mutation of A773 and G774 to G773 and A774 (shown in italics).

the RNA helices and binding of additional Gag polyproteins.[20,29] Where and when complete coating of the viral RNA by Gag or its cleavage products occurs is as yet unknown although there is evidence that the centrosome is a critical encapsidation site.[30]

Binding of the mature cleaved NC to SL3 has been assessed using a selection of different assays including filter binding, NMR, fluorescence quenching, mass spectrometry, and gel mobility shift.[27,31–35] However, these approaches only enable estimation of NC binding affinity to the terminal tetra-loop sequence and offer limited insight into the Gag binding mechanism, which leads to encapsidation of the viral genome.

Deletion and mutation studies consistently identify SL3 as the major component of Ψ.[20,27,33–36] However, a higher affinity for NC was demonstrated by the SL2 sequence compared to the SL3 tetra-loop sequence,[36] which suggests that there are potential additional contributions from the viral RNA sequence surrounding the SL3 tetra-loop during Gag binding in vivo. This is significant for SL3 because the extended helix we and others identified containing an internal RNA loop[37–39] which we have consistently detected by use of biochemical probing[29,38] and shown to be metastable,[29] is not represented in the loop RNAs used in many of the studies to date although recent work describing two alternative structures for the HIV-1 leader includes the internal loop in one of the predicted structures.

To attempt to clarify the mechanism of Gag binding to Ψ, we have developed an *in vitro* assay involving inhibition of Gag-RNA binding by antisense ON analogues targeted to SL3 (reviewed in[3,4]). ON-RNA binding was confirmed to occur at the predicted sequence and the remaining RNA folding was unaltered upon ON binding. This is in contrast to the expected effect of deletion mutants. The effect of hyperstabilisation of the SL3 stem loop by mutation to a GNRA tetra-loop was also investigated given the evidence of conserved metastability in SL3 and published data suggesting the flexibility in SL3 is important.[40] Our analyses show that SL3 contains a secondary binding site for Gag other than the terminal tetra-loop and demonstrate that steric block ONs are effective tools for determining RNA-protein interactions.

MATERIALS AND METHODS

Oligonucleotide Analogues

2′-*O*-Methyl (2′Ome) and phosphorothioate-linked 2′Ome (2′Ome/PS) ONs were commercially produced (Dharmacon). 2′Ome/locked nucleic acid mixmer (2′Ome/LNA) ONs were synthesized by the MRC Laboratory of Molecular Biology (Cambridge, UK). The ONs are summarized in Table 1. The first number indicates the length of the ON (e.g., 12m1 is

TABLE 1 Sequences of ONs tested

ON Chemistry	ON Name	Sequence (5′–3′) and Composition	Target sequence	Binding to RNA	Affinity (nM)
2′Ome	12m1	UAGUCAAAAUUU	757–768	−	
	12m2	CCGCUAGUCAAA	761–772	−	
	12m3	GCCUCCGCUAGU	765–776	+	nd
	12m4	UCUAGCCUCCGC	769–780	+	nd
	12m5	UCCUUCUAGCCU	773–784	−	
	12m6	UCUCUCCUUCUA	777–788	−	
	12m3.5	UAGCCUCCGCUA	767–778	+	nd
	14m3	UAGCCUCCGCUAGU	765–778	+	235
	14m3.5	UCUAGCCUCCGCUA	767–780	+	nd
	16m3	UCUAGCCUCCGCUAGU	765–780	+	170
	12mR	GGGAAUCUGACC	–	−	
2′Ome/PS	p14m3	U.A.G.C.C.U.C.C.G.C.U.A.G.U	765–778	+	840
	p16m3	U.C.U.A.G.C.C.U.C.C.G.C.U.A.G.U	765–780	+	290
	p16mMm	U.C.U.A.G.C.C.*C.G.U.C.*C.U.A.G.U	–	–	
	p16mScr	C.U.G.U.C.A.C.C.U.G.U.C.A.U.C.G	–	−	
2′Ome/LNA	L14m3	U**A**G**C**C**U**C**G**C**U**A**G**U	765–778	+	80
	L16m3	U**C**U**A**G**C**C**U**C**C**G**C**U**A**G**U**	765–780	+	75
	L16mSL3mut	U**C**U**A**G**C**U**C**C**C**G**C**U**A**G**U**	765–780	+	500
	L16mMm	U**C**U**A**G**C**C*C.G.U.C*C**U**A**G**U**	–	–	
	L16mScr	C**U**G**U**C**A**C**C**U**G**U**C**A**U**C**G**	–	−	

All of the ONs that were targeted to the SL2 region of Ψ are indicated by the designation SL2. All the other ONs targeted the SL3 region of Ψ. Control ONs are random (R), mismatched (Mm–with mismatched bases shown in italic) and scrambled (Scr).

Successful binding of ONs to ΔA1 RNA and the relative affinities are indicated.

Key: Upper case = 2′Ome nucleosides; bold and underlined = LNA nucleosides; full stop (period) = PS linkage; nd = not done.

a 12mer). The last figure is the relative position of the 3′ end of the ON on the RNA target structure shown in Figure 1 (e.g., 12m1 binds 5′ on the target RNA to 12m2, etc). The chemical nature is indicated by the font and presence or absence of full stops (periods). Further explanation can be found in the legend to Table 1.

RNA Preparation

The KS1620ΔA1 plasmid was previously constructed by inserting the *BglII* fragment (nucleotides 474-2095) from the HIV-1 HXBc2 sequence (accession number AF033819), containing the 53bp ΔA1 deletion (nucleotides 690–734),[20] into Bluescript KSII (Stratagene). KSGGGA contains the same *BglII* fragment with nucleotides 772 and 773 mutated from AG to GA. PCR of the ΔA1 DNA template for transcription was carried using the KS1620ΔA1 plasmid with forward primer (5′-AATACGACTCACTATAGGAAACCAG AGGAGC-3′) and reverse primer (5′-CTCTCTCCTTCTAGCCTCCGC-3′). PCR of the GGGA DNA template for transcription was carried out using the KS1620GGGA plasmid with forward primer (5′-TAAATACGACTCACTATAGGCGACTGGTG-3′) and reverse primer (5′-GCACCC ATCTCTCTCCTTCTAGC-3′). Radioactively labelled RNA was produced using α^{32}P UTP (Amersham Biosciences) and the Riboprobe System Kit (Promega) as per manufacturers' instructions.

Primer Extension Analysis

30pmol ΔA1 RNA was annealed to reverse primer RP1 (5′ CTAATTCTC-CCCCGC 3′, 50 pmol), with or without 2′ O-methyl/LNA mixmer ON (10 pmol) in a 5 μl reaction containing 12 mM Tris pH 7.5 and 20 mM KCl. For annealing, the reaction mix was denatured at 70°C for 1 minute then slowly cooled to 42°C. 2μl of the annealed RNA/primer was added to 3 μl of a mix containing 7.5 mM Tris pH8.3, 30 mM KCl, 7.5 mM $MgCl_2$, 6 mM DTT, 0.3 mM each of dGTP, dATP, dCTP, 3 μM dTTP, 2 μCi [α^{32}P]-dTTP (10 mCi/ml; Amersham Biosciences), 8U RNase inhibitor RNasin (Promega) and 5U AMV reverse transcriptase (Promega). After incubation at 42°C for 15 minutes, 1 μl of 1.8 mM dTTP was added and incubation continued for a further 15 minutes. The reaction was stopped with 6 μl loading buffer II (Ambion) and heated at 80°C for 5 minutes. Samples were then analyzed on a 10% (w/v) polyacrylamide gel in addition to a sequence ladder generated using standard dideoxy sequencing from the same primer used for primer extension (RP1) on the KS1620ΔA1 plasmid template in a cycle sequencing reaction (*fmol* DNA cycle sequencing system, Promega). The direct incorporation method was employed, using [α^{32}P]-dTTP. Gels were analyzed by autoradiography.

Ribonuclease Sensitivity

30 pmol ΔA1 RNA, with or without 2′ O-methyl/LNA mixmer ON (10 pmol), was heated at 70°C for 1 minute and cooled slowly to room temperature, in a 5 μl reaction containing 2 μl of 10 × structure buffer for RNase T_1/V_1 digestion (Ambion). The RNA/oligonucleotide mixture was subjected to RNase T_1 (Ambion) or RNase V_1 (Ambion) digestion as per manufacturer's instructions. RNA was precipitated in 2 volumes of precipitation/inactivation buffer (Ambion) and washed with 70% ethanol. Pellets were resuspended in 4 μl nuclease free water, and 2 μl used for primer extension analysis.

Electrophoretic Mobility Shift Assays (EMSA)

EMSAs were carried out in a 20 μl reaction mix containing 74.5 nM labelled target RNA (determined by TCA precipitation), varying concentrations of ON and/or GST-Gag-1 (full length Gag polyprotein prepared as described in[41]), 50 mM $MgCl_2$, 4 μg yeast tRNA and 1× binding buffer (50 mM KCL, 50 mM Tris-Cl,). In RNA-ON only EMSAs the reaction mix was heated at 95°C for 3 minutes, snap cooled on ice, and incubated at room temperature for 20 minutes. In RNA-Gag only EMSAs the reaction mix (minus Gag) was heated at 95°C for 3 minutes and snap cooled on ice. Gag was then added and incubated at room temperature for 20 minutes. In RNA-ON-Gag EMSAs the reaction mix (minus Gag) was heated at 95°C for 3 minutes, snap cooled on ice, and incubated at room temperature for 20 minutes. Gag was then added and incubated for a further 20 minutes at room temperature. ON binding was similar in these conditions and in those used for primer extension. The incubation step was followed by the addition of 10 μl of 10x native loading buffer (Ambion), and 10 μl of the mix was then electrophoresed on a 10% polyacrylamide gel (Readygel; Biorad) in 1× TBE (89 mM Tris-borate, 2 mM EDTA, pH 8.3) at 4°C. The gel was dried onto filter paper and RNA analyzed on x-ray film and a real time Instant Imager (Packard).

RESULTS

Oligonucleotide Binding to Ψ RNAs

The RNA used in this study consisted of a truncated HIV-1 Ψ sequence (Figure 1A). Preliminary studies showed that the wild type sequence had the same binding characteristics as an RNA containing the complete SL1–3 region but in the latter it was more difficult to distinguish unbound and oligonucleotide-bound RNA because of their similarity in size (data not shown). Use of a truncated RNA containing most of the SL2, and the

complete SL3, sequence solved this problem. Previous studies have shown weak binding of NC to SL1 and SL4, which suggested that these regions are not involved in an initial high affinity binding interaction with Gag during encapsidation. Removal of the SL1 kissing loop sequence also eliminated any confusion arising from RNA dimer formation. ΔA1 contained the wild type GGAG SL3 terminal tetra-loop sequence. The GGGA mutant represented a GNRA mutated tetra-loop sequence (Figure 1B).

An array of ONs was synthesized, based on three different chemistries: 2′-*O*-Methyl (2′Ome), phosphorothioate-linked 2′Ome (2′Ome/PS) and 2′Ome/locked nucleic acid mixmer (2′Ome/LNA) ONs [42] (Table 1). 12mer 2′Ome ONs were designed to span the entire ΔA1 SL3 sequence, two of which bound the RNA, 12m3 and 12m4. These indicated the most susceptible sites for strand invasion and further ON studies were based on these sites. Alteration of the composition and size of ON based on 12m3 and 12m4 led to the production of high affinity ONs complementary to SL3 encompassing the terminal tetra-loop sequence. Within these higher affinity ONs, three groups emerged; two ONs: p14m3 and p16m3 (2′Ome/PS) displayed the lowest affinities at 840 nM and 290 nM, respectively (Figures 2A and 2D); two ONs: 14m3 and 16m3 (2Ome) showed affinities of 235 nM and 170 nM respectively (Figures 2B and 2D); and two additional ONs: L14m3 and L16m3 (2′Ome/LNA mixmer) showed the highest affinities at 80nM and 75nM respectively (Figures 2C and 2D).

A high affinity 2′Ome/LNA ON was designed complementary to the GGGA mutant SL3 sequence (L16mSL3mut) and showed a lower binding affinity, 500 nM, compared with its counterpart designed complementary to the wild type SL3 (Table 1). The ONs were identical in composition and target position on the RNA, and the reduced binding affinity of GGGA binding ON thus represented a reduced strand invading ability caused by the well-documented stable GNRA loop structure.[40]

Specificity of ON Binding

Reverse primer extension analysis across the packaging signal template has previously been shown to create a series of pausing products due to the existence of natural pausing sites for the reverse transcriptase enzyme, which correlate with known structure and sequence motifs.[43] Primer extension analysis was used to analyze the natural pausing pattern of reverse transcriptase on ΔA1 RNA, with and without bound ON. Figure 3A shows that binding of both L14m3 and L16m3 SL3-targeted ONs caused a large pause on the sequence of SL3 bound by the ONs. The pause length corresponded to the length of the ON used, with a longer pause seen for L16m3. The pause profile corresponds to the site of encounter of the duplex by the RT enzyme and the RT footprint itself hence the footprint approximates to the sequence bound by the oligo. No pauses were

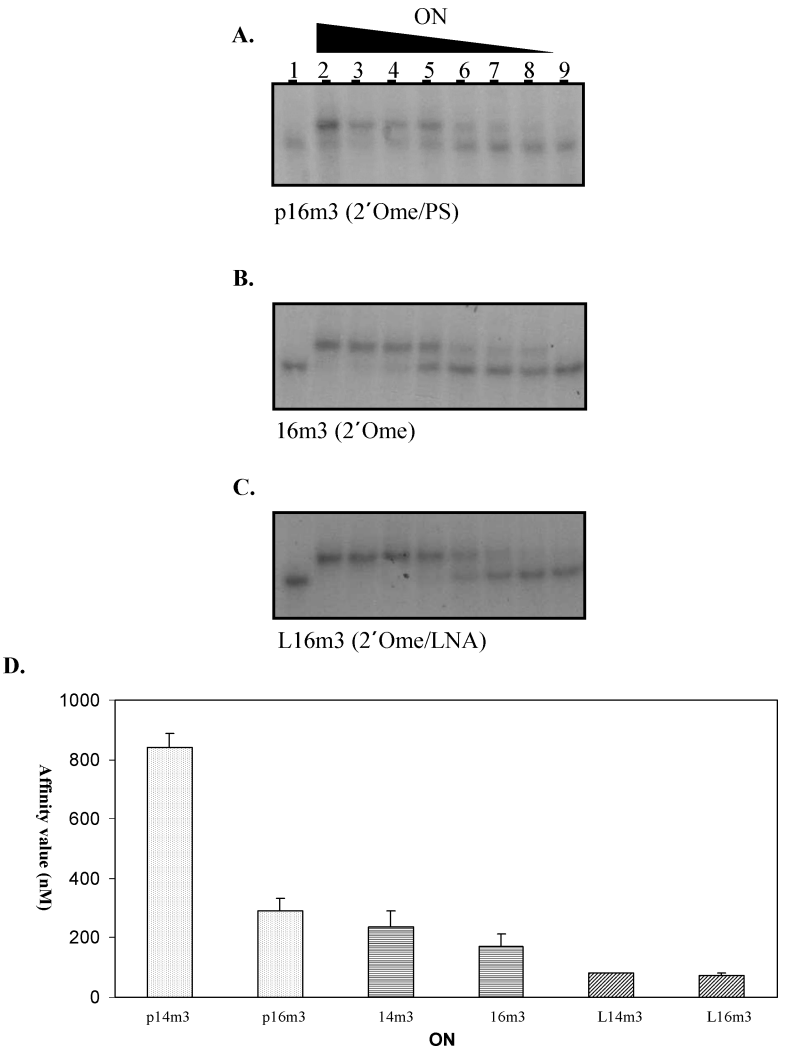

FIGURE 2 ON affinity values for ΔA1 RNA. (A) PAGE analysis of binding assays of ΔA1 RNA and titrating of p16m3 ON. Lane order: 1, no ON; 2, 1280 nM ON; 3, 640 nM ON; 4, 320 nM ON; 5, 160 nM ON; 6, 80 nM ON; 7, 40 nM ON; 8, 20 nM ON; 9, p16mScr ON 2000 nM. (B) As (A) using 16m3 ON with the exception of 12mR present in lane 9. (C) As (A) using L16m3 ON with the exception of L16mScr in lane 9. (D) Summary of affinity values of 14mers and 16mers of all analogue ONs tested.

observed in the presence of L16mScr ON. No additional pauses were seen on the L14m3 or L16m3 bound RNA demonstrating that the ON binding is sequence specific. Moreover, apart from the ON-bound region, the overall pausing pattern was essentially unchanged when compared with unbound RNA, suggesting that the RNA structure away from the binding site was unaltered.

RNA Structure Mapping

The ΔA1 RNA was preincubated in the presence or absence of ON binding and then treated with either RNase T_1 and RNase V_1. RNase T_1 treatment cleaves internucleotide bonds 3′ of unpaired G residues and, during primer extension, results in reverse transcriptase pausing. As expected, RNase T_1 cleaved G^{771} and G^{772} in the SL3 tetra-loop region on unbound RNA or in the presence of L16mScr (Figure 3B). However, binding of SL3-targeted ONs inhibited this cleavage, indicating that RNase T_1 was unable to cleave due to the double-stranded nature of the ON-bound RNA. Cleavage also occurred at G^{764} in the presence and absence of ON suggesting that ON binding to A^{765} does not hinder the availability of the G residue for cleavage. Compared to RNA only, no additional RNase T_1 cleavage sites were observed on ON-bound RNAs.

Reverse transcriptase pausing is also induced at RNase V_1 cleavage sites which cleaves internucleotide bonds at helical regions. On the RNA template, cleavages were consistently detected in the SL3 stem region 5′ of the tetra-loop (C^{766}UAGC), and also possibly at the base of the modified SL2 stem region (C^{751}GC) and in the non-canonical helix at the base of SL3 (A^{781}GGA) (Figure 3C). Upon SL3-targeted ON binding these cleavages were still present and no additional cleavages were observed. The ribonuclease sensitivity data therefore provide strong evidence that the binding of SL3-targeted ONs to the ΔA1 RNA did not induce a major change in global RNA folding.

Gag-RNA Binding

Gag-GST preparations were normalized between experiments by SDS-PAGE analysis to determine protein concentration. Gag was titrated against constant concentrations of RNA and analyzed for binding by polyacrylamide electrophoresis gel electrophoresis (PAGE). Gag-RNA complexes migrated more slowly, as seen in Figure 4. Relative Gag-RNA binding affinities were calculated and varied between 4 and 6 μM for different preparations (data not shown). Control EMSAs using GST protein only, showed absence of non-specific binding of the GST element of the fusion protein (Figure 4, lane 5).

Gag-ΔA1 RNA Binding +/− SL3 Targeted ON

Each of the SL3 targeted ONs was pre-incubated with ΔA1 RNA at a concentration that resulted in 100% binding (2 μM) and then incubated with decreasing concentrations of Gag. Gag binding was visibly reduced by all of the high affinity ONs tested (for example L16m3, Figure 5A). Relative binding affinities for Gag were calculated in the presence of ON and plotted

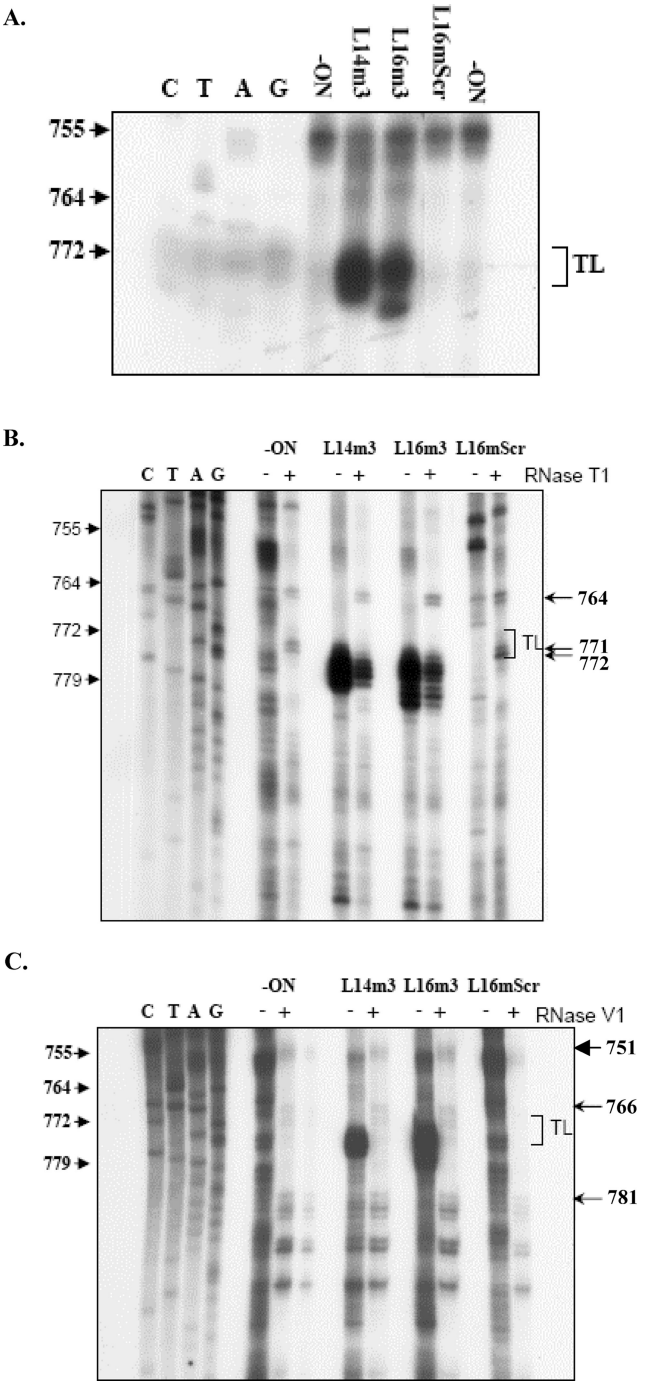

FIGURE 3 ON binding and RNA structure in the presence of modifying enzymes. (A) Modification of ΔA1 RNA +/− 2′O′me/LNA ON binding by RNase T1 digestion. (B) Modification of ΔA1 RNA +/− 2′Ome/LNA ON binding by RNase V1 digestion. Lanes between ON+ and L14m3 are empty. (CTAG = sequencing ladder. TL = tetra-loop on SL3. Arrows indicate enzyme specific cleavage.

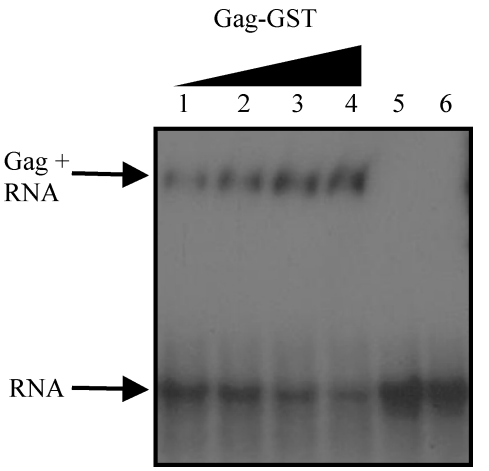

FIGURE 4 Gag-GST and ΔA1 RNA binding. A. PAGE analysis of RNA and Gag-GST/GST binding. Lane order: 1–4, 3.26 μM, 3.74 μM, 4.23 μM, 4.71 μM Gag-GST respectively; 5, 4.71 μM GST; 6, no protein.

relative to control binding in the absence of ON (Figure 5B). The reduction of Gag binding varied according to the size and composition of the ON and correlated closely with the affinity of the ON for RNA. PS linked ONs p14m3 and p16m3 showed the least effect, reducing Gag binding to 0.81 and 0.71 relative to controls (given a value of 1.0) (Figure 5B). 2′Ome and 2′Ome/LNA ONs greatly reduced Gag binding, with levels at 0.16, 0.21, 0.23 and 0.15 for 14m3, 16m3, L14m3, and L16m3 ONs, respectively (Figure 5B). Inhibition of Gag binding was sequence specific, with control ONs of four mismatched nucleotides, or a scrambled sequence, showing no RNA binding themselves and no competition for Gag binding (data not shown).

Gag-GGGA Mutant RNA Binding

An SL3 mutant RNA identical to ΔA1 except for an alteration of the tetra-loop from GGAG to GGGA was used. This was designed to produce a hyperstable GNRA loop at SL3, which maintained the purine composition. SL4 of ψ is an example of a GNRA loop and has a 100 fold lower affinity for Gag than SL3.[32] The GGGA mutant RNA was investigated for Gag binding in the absence of ON and in the presence of L16mSL3mut ON which is complementary to the mutated purine loop.

Gag binding to the mutant RNA in the absence of ON was reduced to 0.56, which confirmed the importance of the GGAG tetra-loop sequence in specific recognition of Gag (Figure 6). Although Gag showed impaired binding to the mutant RNA, the reduction was not as marked as when SL3 targeted ON was bound to ΔA1 RNA, suggesting Gag binding to SL3 was still able to bind to some extent the mutant tetra-loop sequence. This is the likely

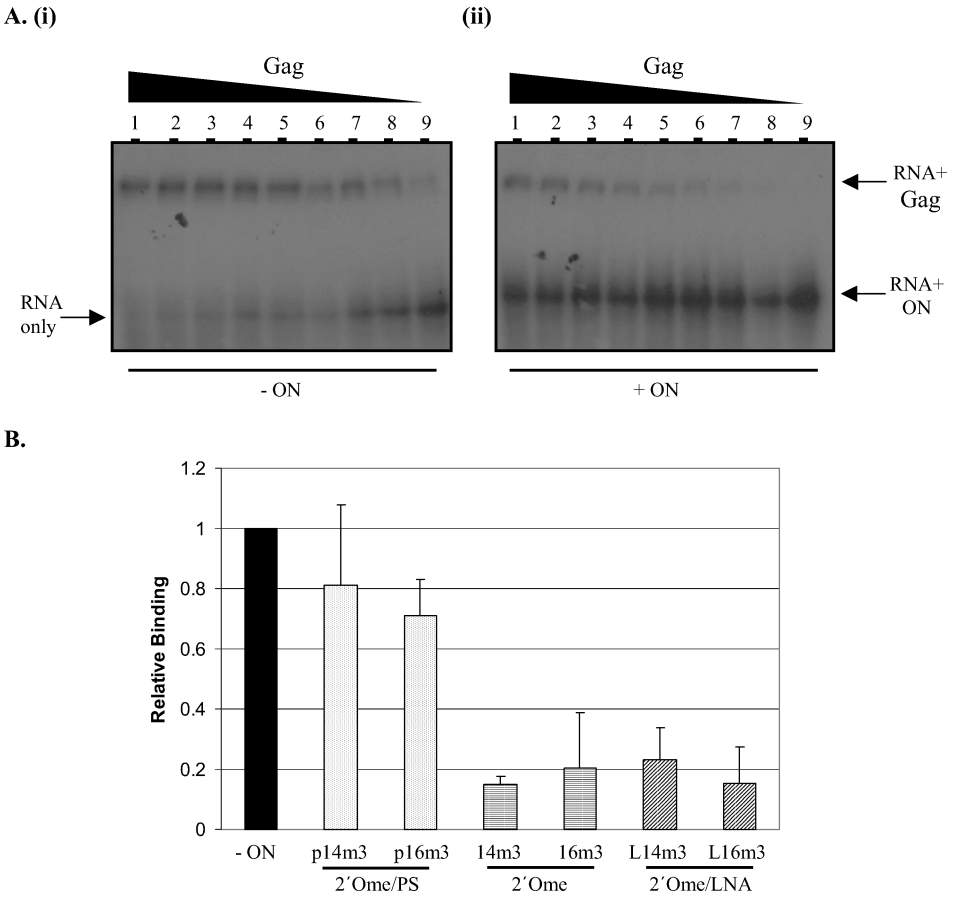

FIGURE 5 SL3 ON inhibition of Gag binding. A. (i) and (ii) Binding of ΔA1 RNA with decreasing Gag in the absence (i) and presence (ii) of L16m3 (2 μM). Lane orders: 1, 4.71 μM Gag; 2, 4.23 μM Gag; 3, 3.74 μM Gag; 4, 3.26 μM Gag; 5, 2.76 μM Gag; 6, 2.27 μM Gag; 7, 1.79 μM Gag; 8, 1.3 μM Gag; 9, 0.81 μM Gag. B. Gag binding in the presence of SL3 targeted ON, measured as a fraction of wild type Gag binding (−ON).

source of Gag binding to the mutant RNA, since this loop was bound by SL3 targeted ONs in addition to the GGAG tetra-loop. With L16mSL3mut ON bound to the mutant RNA, Gag binding efficiency was measured as 0.16, compared with 0.15 from ΔA1 with L16m3 bound (Figure 6B) implicating the internal loop of SL3 as a potential binding site for Gag on the RNAs analyzed. Oligos targeted to SL2 did not reduce this further (data not shown).

DISCUSSION

The aims of this study were to identify ONs with high affinity for Ψ RNA, to investigate the mechanism of binding and to examine the effectiveness of high affinity ONs in determining the process of encapsidation

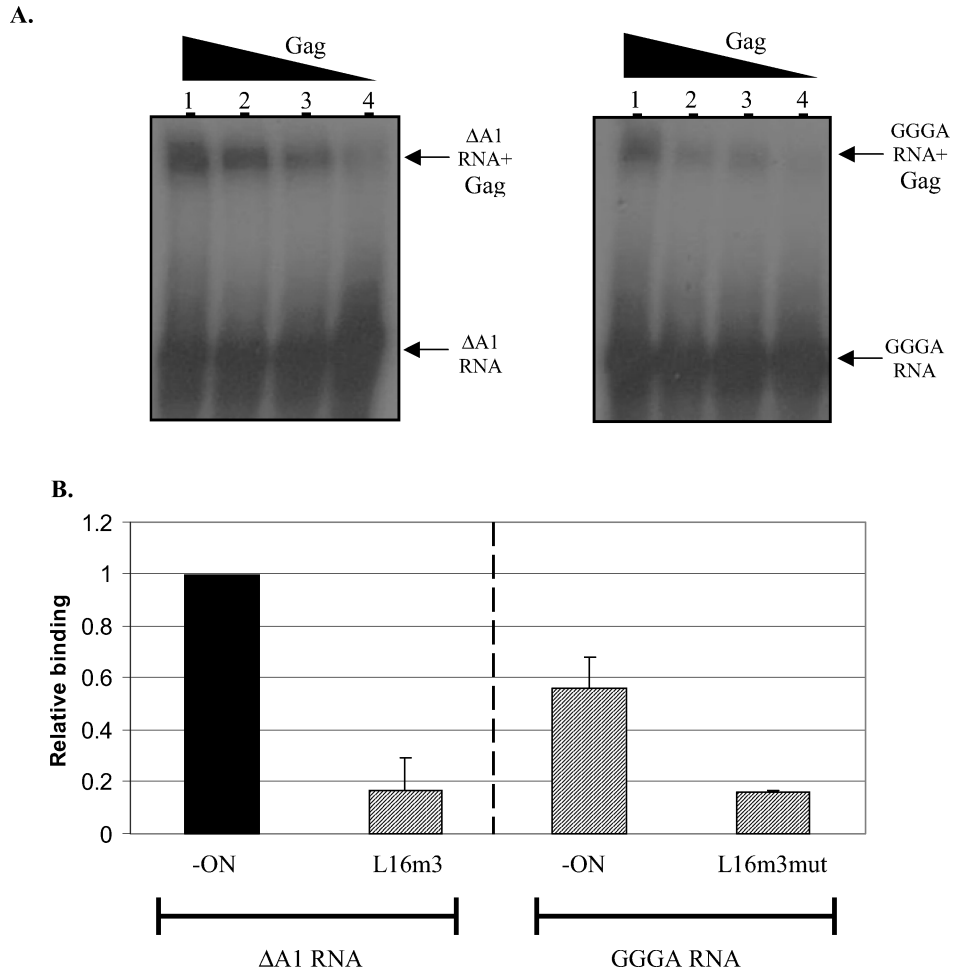

FIGURE 6 Gag binding to ΔA1 RNA and GGGA mutant RNA. (A) Titrating Gag binding to (i) ΔA1 RNA and (ii) GGGA mutant RNA in the absence of ON. Lane order: 1, 4.71 μM Gag; 2, 4.23 μM Gag; 3, 3.74 μM Gag; 3.26 μM Gag. (B) Graphical representation of Gag binding to ΔA1 and GGGA RNAs in the presence of sequence specific SL3 2′Ome/LNA ONs.

via Gag protein binding to the SL3 region. A large range of ONs based on three chemistries (2′Ome/PS, 2′Ome, 2′Ome/LNA) helped to identify optimum targets for high ON affinity binding. Interestingly, minor changes in the ON binding site had marked effects, with 12mer3 and 12mer4 ONs (2′Ome) showing binding, and the immediate flanking ONs that are only 4 nucleotides different. The variations strongly implicate ease of invasion of the different RNA structures as a critical factor.[44,45] In targeting SL3, preferential binding of 12mer3 and 12mer4 ONs rather than 12mer1, 2, 5 and 6 ONs might be predicted from the presence of an internal metastable loop.[29,46] The presence of this loop, in the context of a larger RNA, is

confirmed by the susceptibility to strand invasion by the 3′- end of the 12mer 3 and 12mer4 ONs.

As expected, the ONs bound to the predicted RNA target sequences confirming their high specificity. Further RNA structural analyses also revealed that global RNA folding was not altered upon ON binding. To our knowledge, this is the first study to show that high affinity ONs possess this ability, which has major implications for their use as *in vitro* RNA-protein binding inhibitors. Until now, deletion mutants have been widely used to identify putative protein binding sites on RNA.[20,27,33–36] However, they run the risk that major alterations of RNA sequence can grossly affect RNA secondary structure, which is essential for many protein-RNA interactions, including Gag-Ψ. With the availability of these high affinity binding reagents capable of inhibiting protein binding, RNA can be probed for protein binding sites without affecting native secondary RNA structures. Our probing data suggest that short stem loop sequences other than those involved in the heteroduplex in longer sequences tertiary and long range interactions would complicate analysis.

In addition to confirming the presence of an internal metastable loop in SL3, the two different RNAs used enabled investigation of the mechanism of Gag binding. The tetra-loop was confirmed as the major nucleation site on SL3. Binding SL3 with ON markedly reduced the RNA-Gag interaction, possibly by specific inhibition of Gag binding to the high affinity tetra-loop sequence.[27,34,35] As previously reported,[29] the structure of the RNA is also likely to be altered upon Gag binding, which would be prevented by ON binding to SL3. Stabilisation of the SL3 RNA structure was tested with a GNRA loop mutation. The reduction in Gag binding to the mutant RNA would also suggest that for efficient Gag binding to occur, interaction must take place at the SL3 tetra-loop, followed by unwinding of the RNA double helix. The importance of internal metastability in SL3 may explain the lower affinity for NC detected by Shubsda,[35] as in their study an RNA containing a stable helix subtended the SL3 purine loop.

Another putative Gag binding site identified here is the internal loop of SL3. This observation was made through analysis of Gag binding to the GGGA mutant in the presence and absence of ON, and is consistent with footprinting studies carried out on Ψ.[29] Gag binding to the metastable internal loop on Ψ could be a consequence of SL3 tetra-loop binding opening up the RNA structure, promoting Gag binding. However, Gag binding to the internal loop on the GGGA mutant suggests that this is not the case and that the internal loop is an independent binding site for Gag since minimal Gag binding and unwinding of the RNA structure is occurring at the tetra-loop.

In addition to being one of the few studies that involve investigation of binding to RNA of the full-length Gag polyprotein, the SL3 stem loop has here been analyzed in the context of a more complete Ψ sequence. High

affinity ON analogue binding has confirmed that SL3 is the principal binding region for Gag, containing two binding sites. This study has validated high affinity steric block ONs as sequence specific molecules, capable of: (1) binding to RNA without altering native secondary structure; and (2) probing an RNA sequence for putative protein binding sites. The ability of these ONs to inhibit Gag binding is also encouraging for these ONs to be investigated as molecular tools in cells or as anti-HIV therapeutics.[16,47]

REFERENCES

1. Kurreck, J., et al. Design of antisense oligonucleotides stabilized by locked nucleic acids. *Nucleic Acids Res.* **2002**, 30(9), 1911–1918.
2. Crooke, S.T., et al. Kinetic characteristics of Escherichia coli RNase H1: cleavage of various antisense oligonucleotide-RNA duplexes. *Biochem. J.* **1995**, 312(Pt. 2), 599–608.
3. Kurreck, J. Antisense technologies. Improvement through novel chemical modifications. *Eur. J. Biochem.* **2003**, 270(8), 1628–1644.
4. Petersen, M.; Wengel, J. LNA: a versatile tool for therapeutics and genomics. *Trends Biotechnol.* **2003**, 21(2), 74–81.
5. Mercatante, D.R.; Mohler, J.L.; Kole, R. Cellular response to an antisense-mediated shift of Bcl-x pre-mRNA splicing and antineoplastic agents. *J. Biol. Chem.* **2002**, 277(51), 49374–49382.
6. Michel, T., et al. Cationic phosphoramidate alpha-oligonucleotides efficiently target single-stranded DNA and RNA and inhibit hepatitis C virus IRES-mediated translation. *Nucleic Acids Res.* **2003**, 31(18), 5282–5290.
7. Kaushik, N., et al. Anti-TAR polyamide nucleotide analog conjugated with a membrane-permeating peptide inhibits human immunodeficiency virus type 1 production. *J. Virol.* **2002**, 76(8), 3881–3891.
8. Boulme, F., et al. Modified (PNA, 2′-O-methyl and phosphoramidate) anti-TAR antisense oligonucleotides as strong and specific inhibitors of in vitro HIV-1 reverse transcription. *Nucleic Acids Res.* **1998**, 26(23), 5492–5500.
9. Darfeuille, F., et al. 2′-O-methyl-RNA hairpins generate loop-loop complexes and selectively inhibit HIV-1 Tat-mediated transcription. *Biochemistry* **2002**, 41(40), 12186–12192.
10. Darfeuille, F., et al. LNA/DNA chimeric oligomers mimic RNA aptamers targeted to the TAR RNA element of HIV-1. *Nucleic Acids Res.* **2004**, 32(10), 3101–3107.
11. Holmes, S.C.; Gait, M.J. The synthesis of 2′-O-methyl G-clamp containing oligonucleotides and their inhibition of the HIV-1 Tat-TAR interaction. *Nucleosides Nucleotides Nucleic Acids* **2003**, 22(5–8), 1259–1262.
12. Arzumanov, A., et al. Inhibition of HIV-1 Tat-dependent trans activation by steric block chimeric 2′-O-methyl/LNA oligoribonucleotides. *Biochemistry* **2001**, 40(48), 14645–14654.
13. Leeds, J.M., et al. Pharmacokinetics of a potential human cytomegalovirus therapeutic, a phosphorothioate oligonucleotide, after intravitreal injection in the rabbit. *Drug Metab. Dispos.* **1997**, 25(8), 921–926.
14. Elayadi, A.N.; Braasch, D.A.; Corey, D.R. Implications of high-affinity hybridization by locked nucleic acid oligomers for inhibition of human telomerase. *Biochemistry* **2002**, 41(31), 9973–9981.
15. Marwick, C. First "antisense" drug will treat CMV retinitis. *JAMA* **1998**, 280(10), 871.
16. Brown, D.E., et al. Inhibition of HIV-1 replication by oligonucleotide analogues directed to the packaging signal and trans-activating response region. *Antivir. Chem. Chemother.* **2006**, 17(1), 1–9.
17. Ivanova, G., et al. Anti-HIV activity of steric block oligonucleotides. *Ann. NY Acad. Sci.* **2006**, 1082, 103–115.
18. Berkowitz, R.D., et al. 5′ regions of HIV-1 RNAs are not sufficient for encapsidation: implications for the HIV-1 packaging signal. *Virology* **1995**, 212(2), 718–723.
19. Lever, A., et al. Identification of a sequence required for efficient packaging of human immunodeficiency virus type 1 RNA into virions. *J. Virol.* **1989**, 63(9), 4085–4087.
20. Harrison, G.P., et al. Functional analysis of the core human immunodeficiency virus type 1 packaging signal in a permissive cell line. *J. Virol.* **1998**, 72, 5886–5896.

21. Laughrea, M.; Jette, L. HIV-1 gemone dimerization: formation kinetics and thermal stability of dimeric HIV-1Lai RNAs are not improved by the 1–232 and 296–790 regions flanking the kissing-loop domain. *Biochemistry* **1996**, 35, 9366–9374.
22. Muriaux, D.; Fosse, P.; Paoletti, J. A kissing complex together with a stable dimer is involved in the HIV-1Lai RNA dimerization process in vitro. *Biochemistry* **1996**, 35(15), 5075–5082.
23. Paillart, J.C., et al. A loop-loop "kissing" complex is the essential part of the dimer linkage of genomic HIV-1 RNA. *Proc. Natl. Acad. Sci. USA* **1996**, 93(11), 5572–5577.
24. Aldovini, A.; Young, R.A. Mutations of RNA and protein sequences involved in human immunodeficiency virus type 1 packaging result in production of noninfectious virus. *J. Virol.* **1990**, 64(5), 1920–1926.
25. Gorelick, R.J., et al. Noninfectious human immunodeficiency virus type 1 mutants deficient in genomi *c* RNA. *J. Virol.* **1990**, 64(7), 3207–3211.
26. Fisher, A.G., et al. A molecular clone of HTLV-III with biological activity. *Nature* **1985**, 316(6025), 262–265.
27. De Guzman, R.N., et al. Structure of the HIV-1 nucleocapsid protein bound to the SL3 psi-RNA recognition element. *Science* **1998**, 279, 384–388.
28. Rumlova-Klikova, M., et al. Analysis of Mason-Pfizer monkey virus Gag domains required for capsid assembly in bacteria: role of the N-terminal proline residue of CA in directing particle shape. *J. Virol.* **2000**, 74(18), 8452–8459.
29. Zeffman, A., et al. The major HIV-1 packaging signal is an extended bulged stem loop whose structure is altered on interaction with the Gag polyprotein. *J. Mol. Biol.* **2000**, 297(4), 877–893.
30. Poole, E., et al. HIV-1 Gag-RNA interaction occurs at a perinuclear/centrosomal site; analysis by confocal microscopy and FRET. *Traffic* **2005**, 6(9), 741–755.
31. Amarasinghe, G.K., et al. NMR structure of the HIV-1 nucleocapsid protein bound to stem-loop SL2 of the psi-RNA packaging signal. Implications for genome recognition. *J. Mol. Biol.* **2000**, 301(2), 491–511.
32. Amarasinghe, G.K., et al. Stem-loop SL4 of the HIV-1 psi RNA packaging signal exhibits weak affinity for the nucleocapsid protein. structural studies and implications for genome recognition. *J. Mol. Biol.* **2001**, 314(5), 961–970.
33. Clever, J.; Sassetti, C.; Parslow, T.G. RNA secondary structure and binding sites for gag gene products in the 5′ packaging signal of human immunodeficiency virus type 1. *J. Virol.* **1995**, 69(4), 2101–2109.
34. Hagan, N.; Fabris, D. Direct mass spectrometric determination of the stoichiometry and binding affinity of the complexes between nucleocapsid protein and RNA stem-loop hairpins of the HIV-1 Psi-recognition element. *Biochemistry* **2003**, 42(36), 10736–10745.
35. Shubsda, M.F., et al. Affinities of packaging domain loops in HIV-1 RNA for the nucleocapsid protein. *Biochemistry* **2002**, 41(16), 5276–5282.
36. Paoletti, A.C., et al. Affinities of the nucleocapsid protein for variants of SL3 RNA in HIV-1. *Biochemistry* **2002**, 41(51), 15423–15428.
37. Baudin, F., et al. Functional sites in the 5′ region of human immunodeficiency virus type 1 RNA form defined structural domains. *J. Mol. Biol.* **1993**, 229, 382–397.
38. Harrison, G.P.; Lever, A.M.L. The human immunodeficiency virus type 1 packaging signal and major splice donor region have a conserved stable secondary structure. *J. Virol.* **1992**, 66(7), 4144–4153.
39. Hayashi, T.; Ueno, Y.; Okamoto, T. Elucidation of a conserved RNA stem-loop structure in the packaging signal of human immunodeficiency virus type 1. *FEBS Lett.* **1993**, 327(2), 213–218.
40. Heus, H.A.; Pardi, A. Structural features that give rise to the unusual stability of RNA hairpins containing GNRA loops. *Science* **1991**, 253(5016), 191–194.
41. Myers, E.L.; Allen, J.F. Tsg101, an inactive homologue of ubiquitin ligase e2, interacts specifically with human immunodeficiency virus type 2 gag polyprotein and results in increased levels of ubiquitinated gag. *J. Virol.* **2002**, 76(22), 11226–11235.
42. Arzumanov, A., et al. Inhibition of HIV-1 Tat-dependent trans activation by steric block chimeric 2′-O-methyl/LNA oligoribonucleotide*s*. *Biochemistry* **2001**, 40(48), 14645–14654.
43. Harrison, G.P., et al. Pausing of reverse transcriptase on retroviral RNA templates is influenced by secondary structures both 5′ and 3′ of the catalytic site. *Nucleic Acids Res.* **1998**, 26, 3433–3442.
44. Jakobsen, M.R., et al. A genomic selection strategy to identify accessible and dimerization blocking targets in the 5′-UTR of HIV-1 RNA. *Nucleic Acids Res.* **2004**, 32(7), e67.

45. Ooms, M., et al. Probing alternative foldings of the HIV-1 leader RNA by antisense oligonucleotide scanning arrays. *Nucleic Acids Res.* **2004**, 32(2), 819–827.
46. Abbink, T.E., et al. The HIV-1 leader RNA conformational switch regulates RNA dimerization but does not regulate mRNA translation. *Biochemistry* **2005**, 44(25), 9058–9066.
47. Brown, D., et al. Antiviral activity of steric-block oligonucleotides targeting the HIV-1 trans-activation response and packaging signal stem-loop RNAs. *Nucleosides Nucleotides Nucleic Acids* **2005**, 24(5–7), 393–396.